# Plasma properties of laser-ablated Si target in air*

Wang Xiang-Tai ( 王象泰), Man Bao-Yuan ( 满宝元), Wang Gong-Tang ( 王公堂),
Fan Xi-Jun ( 樊锡君), Wang Jun ( 王 军)
(*Department of Physics, Shandong Normal University, Jinan 250014*)
Xu Bing-Zhang ( 许炳璋) and Mei Liang-Mo ( 梅良模)
(*Department of Physics, Shandong University, Jinan 250100*)

**Abstract** In plasma emission spectra produced by pulsed laser ablation of Si target in air, under the assumption of local thermodynamic equilibrium (LTE), the electron temperature and the electron number density are calculated, respectively. It seems that LTE is valid in early stage of the laser induced plasma evolution.

**Keywords** Plasma emission spectra, Laser ablation, Properties of plasma, Time dependence

## 1 Introduction

Recently, much more attentions are paid to the evolution of the laser induced plasma on the target surface[1], since it is important for both the basic understanding of laser-material interactions and many practical applications, for instance, the application of pulsed laser deposition (PLD) for thin film growth[2–4]. Because of the highly transitory behaviour of laser-produced plasma, it is the most important to characterize the laser produced plasma (LPP) in a time- and space-resolved way. Wolf[1] studied the optical emission spectra from LPP on laser-ablated $SiO_2$ surface in vacuum using a time evolution diagnostic technique. In this paper, optical emission spectroscopy is used to characterize the plasma produced by 1.06 $\mu$m, 10 ns pulsed laser ablation of Si target in air. The temporal variation of the intensities of the spectrum lines was analyzed. Under the assumption of local thermodynamic equilibrium (LTE), the electron temperature and the electron number density in the plasma were deduced from the relative line intensity data and the Stark broadening data, respectively. The LTE condition is discussed finally.

## 2 Experiment

The experimental arrangement is shown in Fig.1. A Q-switched Nd:YAG laser (Quanta Ray DCR–3), producing 1.06 $\mu$m radiation in 10 ns pulse widths, was focused onto the surface of Si target with mass fraction of 0.9999 in air. The laser induced plume was imaged to the detecter of EG&G OMA with ISA H320 spectrometer with resolution of 0.01 nm by two lenses. The space- and time-resolved emission spectra of the plume are measured with the same method as Ref.[1]. The measured spectrum data were calibrated in wavelength and intensity carefully. The laser power densities used in the experiment are 1.0~10.0 GW/cm$^2$.

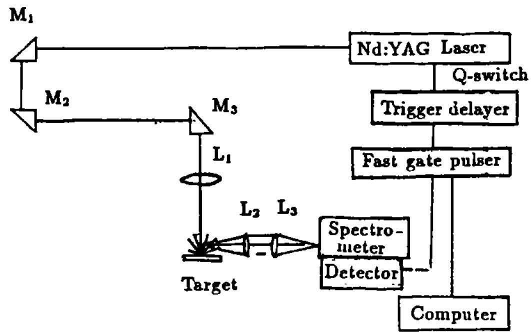


**Fig.1** Schematic diagram of the experimental apparatus

## 3 Results and discussions

### 3.1 Plasma emission evolution

When a target was irradiated by the pulsed laser beam, a bright spark was observed on the target surface, which indicated the ignition of a plasma. Fig.2 shows an evolution

*The Project Supported by National Natural Science Foundation of China and by Natural Science Funds of Shandong Province
Manuscript received date: 1995–11–20

of a continuum emission from the plasma produced on a Si target in the wavelength range of 485~510 nm, which recorded at 1.0 mm from the target surface.

This continuum emission was attributed to both elastic collisions of electrons with ions and atoms (free-free emission) and the recombination of electrons with ions (free-bound emission)[5]. The intensity of the continuum decreases with increase in the delay time. From Fig.2 one finds that there is a very broad peak appearing around 500.5 nm wavelength, which evolves into two narrower peaks when delay time $t_d \geq 150$ ns. The peak is attributed to the singly charged $N^+$ ions in the air plasma. Fig.3 depicts the evolution of the spectrum in $278\,\text{nm} \leq \lambda \leq 292\,\text{nm}$, recorded at the distance of 2 mm from the target surface, with delay time varying from 200 ns to 1800 ns. The isolated lines of the excited neutral Si atoms are clearly identified at $\lambda = 288.15$ nm. As known, the concentration of an electron state of the atoms is proportional to the intensity (the area under its emission line), the area evolution for each isolated identified peak can yield a time-of-flight information for various excited species. As well, the evolution of the relative intensities and the widths of the isolated lines can be used to deduce time-resolved features of the temperature and the number density of the electrons in the plasma as long as the LTE is valid.

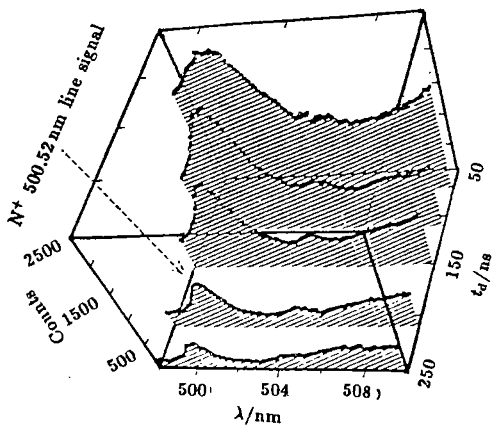


**Fig.2** Spectrum of air plasma on Si target

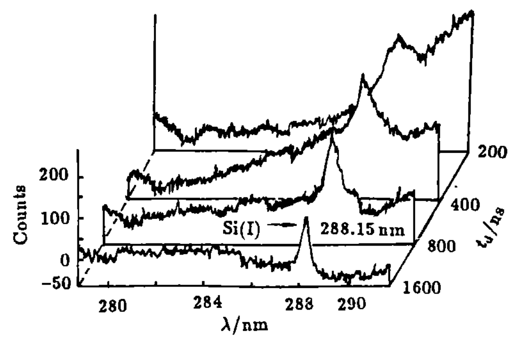


**Fig.3** Evolution of spectral line Si(I) at 288.1 nm

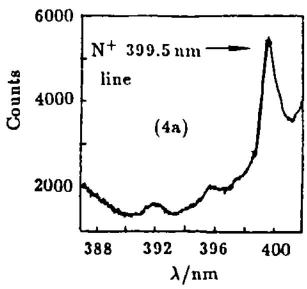


**Fig.4a** Spectral line of $N^+$ at 399.5 nm

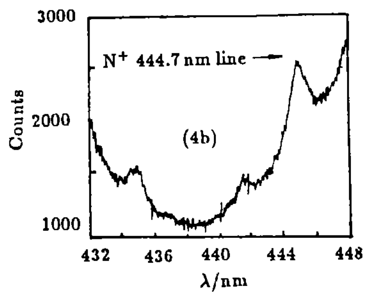


**Fig.4b** Spectral line of $N^+$ at 444.7 nm

### 3.2 Electron temperature

Under the assumption of LTE, the electron temperature in the plasma can be determined by relative line intensity measurements. If one observes two isolated lines, say line 1 and line 2 with central wavelength $\lambda_1$ and $\lambda_2$ respectively, emitting from the same atomic or ionic species, and if the level population are distributed according to the Boltzman law, the relative intensity of these two lines, $\epsilon_1/\epsilon_2$ can be given[5]:

$$\frac{\epsilon_1}{\epsilon_2} = \frac{f_{mn}(1)g_n(1)}{f_{mn}(2)g_n(2)}\left(\frac{\lambda_2}{\lambda_1}\right)^3 \cdot \exp\left[-\frac{E_m(1)-E_m(2)}{KT}\right] \tag{1}$$

where $f_{mn}(i)$ ($i$=1, 2) is the absorption oscillator strength for the transition $m \rightarrow n$, $g_n(i)$ ($i$=1, 2) the statistical weight of the lower level, $E_m(i)$ the energy of the upper energy state $m$

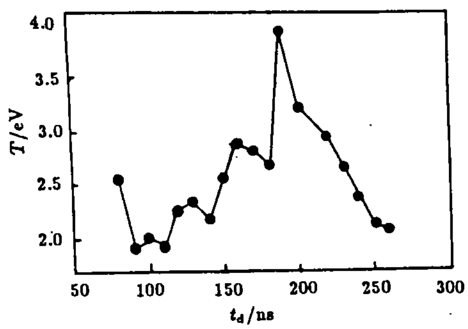


**Fig.5** Electron temperature vs delay time

and $T$ the electron temperature. From Eq.(1) the electron temperature can be determined provided $f_{mn}$, $g_n$ and $E_m$ are known. The atomic spectra data needed in Eq.(1) can be found in Ref.[6]. In this paper we used two $N^+$ ion lines (measured at the distance of 1.0 mm from target surface) at $\lambda$ =399.5 nm and $\lambda$ =444.7 nm to obtain the electron temperature. The two lines are shown in Fig.4. The calculation results are shown in Fig.5. From Fig.5, it can be seen that the electron temperature is about 2.0 eV at 60 ns, and then gradually rises to the peak temperature $T$=3.9 eV at 190 ns, after this cooled to 1.9 eV rapidly.

### 3.3 Electron density

The electron density in the plasma can be calculated from the measurement of the Stark broadening of the isolated lines by using LTE. Fig.4a and Fig.4b shows that the spectral lines are approximately as Lorentzian line shapes, so FWHM of the observed line was corrected by subtracting the contribution by instrumental line broadening using:

$$\Delta\lambda_{\text{real}} = \Delta\lambda_{\text{observed}} - \Delta\lambda_{\text{instrument}} \tag{2}$$

where $\Delta\lambda$ is the full width at half-maximum (FWHM). Fig.6a and Fig.6b are the measured FWHM and wavelength shift of $N^+$ 399.5 nm spectral line versus delay time at 1.0 mm position from target surface.

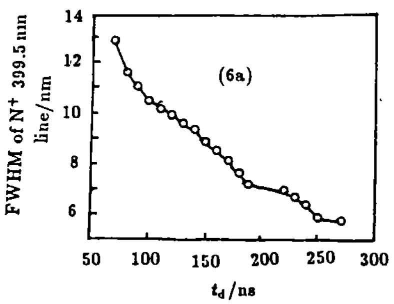


**Fig.6a** FWHM of spectral line 399.5 nm emitted from $N^+$ ion vs delay time

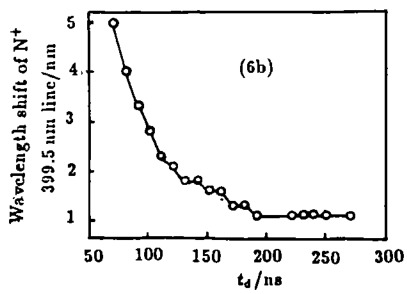


**Fig.6b** The wavelength shift of 399.5 nm ($N^+$) vs delay time

For singly ionized nonhydrogenic ions, the full width at half-maximum, $\Delta\lambda$, is given by[5]:

$$\Delta\lambda_{1/2} = 2W(\frac{N_e}{10^{16}}) + 3.5A(\frac{N_e}{10^{16}})^{1/4}[1 - 1.2N_D^{-1/3}]W(\frac{N_e}{10^{16}})A \tag{3}$$

where the width is in Åand the electron density $N$ is in cm$^{-3}$. The coefficients $W$ and $A$, both independent of density and slowly varying with temperature, are the electron-impact width parameter and the ion-broadening parameter, respectively. The parameter $N_D$ is the number of particles in the Debye sphere as given by:

$$N_D = 1.72 \times 10^9 \frac{[T(\text{eV})]^{3/2}}{[N(\text{cm}^{-3})]^{1/2}} \tag{4}$$

The broadening coefficients $W$ and $A$ can be found in Ref.[7]. The contribution from ion broadening was small, typically less than 0.03 nm for the conditions of this experiment, so the width was mainly due to electron-impact broadening. Using Eqs.(3,4) and the measured Stark broadening data of the 399.5 nm $N^+$ line, the electron density is obtained as shown in Fig.7. From Fig.7, one can find that the electron density is very high in the laser induced air plasma. At $t_d = 90$ ns the density is $7.0 \times 10^{18}$ $cm^{-3}$, and then gradually decays exponentially to $1.0 \times 10^{18}$ $cm^{-3}$.

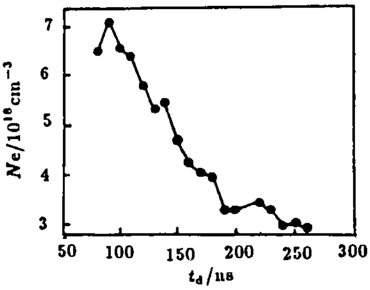


**Fig.7** Electron density vs $t_d$ ($Z$=1 mm)

The high electron density is very favourable for preparing materials in PLD and for LTE to be valid. A necessary condition for LTE is satisfied[8].

$$N \geq 1.4 \times 10^{14} T^{1/2} (\Delta E_{mn})^3 \text{cm}^{-3} \quad (5)$$

where $T$ is the temperature in eV, $\Delta E_{mn}$ the energy difference between the upper and lower states in eV. The highest temperature is $T = 3.9$ eV. Using these values in Eq.(5), we obtained the lowest limit of the electron density of $1.9 \times 10^{15}$ $cm^{-3}$. The value of $N$ obtained from the Stark broadening data is $1.0 \times 10^{18}$ $cm^{-3}$, which is much higher than the lowest limit value. Therefore, it seems that the LTE assumption used in the evaluation of $N$ and $T$ in the early stage of the plasma evolution is valid. However, laser induced plasma is a transitory phenomenon, LTE is only applied to a limited time interval and spacial positions.

Normally, Eq.(3) is valid in the parameter range of $N_D \geq 2$ and $0.05 < A(N_e/10^{16})^{1/4} < 0.5$. Here, we put the obtained temperature $T = 3.9$ eV and $N = 2.5 \times 10^{18} \text{cm}^{-3}$ into Eq.(4) can yield $N_D$ value of 7.2, which is much larger than 2. We have also tested whether the condition $0.05 < A(N_e/10^{16})^{1/4} < 0.5$ is satisfied, and found that it is true.

## 4 Summary

In the early stage of plasma evolution the electron temperature is high to 2~3 eV, and is varying very rapidly. When the time is longer than 190 ns the electron temperature in the plasma is cooled down. The density is as high as $\sim 10^{18} \text{cm}^{-3}$. From our calculation results, it is found that LTE is valid in the early stage of the laser induced plasma evolution.

### References


1 Wolf P J. Appl Phys, 1992; 72(4):1280–1289
2 Wang H, Salzberg A P, Wweiner B R. Appl Phys Lett, 1991; 59:935
3 Izumi H, Ohata K, Sawada T *et al.* Appl Phys Lett, 1991; 59:597
4 Richter A. Thin Solid Films, 1990; 188:275
5 Bekefi G. Principles of laser plasmas. New York: John Wiley and Sons, 1976
6 Wiese W L, Smith M W, Glennon B M. Atomic transition probabilities, Vol.1, hydrogen through neon. Washington D C: National Standard Reference Data System, 1966
7 Griem H I. Plasma spectroscopy. New York: McGraw-Hill, 1964
8 Mcwhirter R W. In: Huddlestone R H, Leonard S L, eds. Plasma diagnostic techniques. New York: Academic, 1965